

**Phase II Final Report Submitted to**  
**Office of Naval Research**  
**Dr. Paul Armistead, Program Manager**

By

**Georgia Institute of Technology**  
Atlanta, Georgia 30332-0400

**MOLECULAR PHOTONICS: HIGH-SPEED MATERIALS FOR  
OPTICAL SIGNAL PROCESSING**

**Technical Point of Contact:**

**Professor Joseph Perry**

School of Chemistry & Biochemistry  
Georgia Institute of Technology  
770 State Street  
Atlanta, GA 30332-0400  
Phone: 404-385-6046  
FAX: 404-385-6057  
Email: [joe.perry@gatech.edu](mailto:joe.perry@gatech.edu)

**This Report Contains Georgia Tech Proprietary Information is for Government Purposes  
Only**

## Phase II Progress

*Progress made toward the development of improved  $\chi^{(3)}$  materials for sensor protection in the 700 – 900 nm range (transmission > 70%, suppression of 20 dB, pulse duration ps –  $\mu$ s)*

### A. Charge-Transfer Composite Films

For this project metric, charge transfer (CT) composites consisting of selected electron-rich, two-photon absorbing conjugated polymers (as donors) and electron-deficient materials (as acceptors) were chosen as candidates for efficient optical limiting materials. In order to ensure that effective CT could occur, films consisting of a high number density of active species had to be fabricated. While a large number of films of various donor and acceptor constituents were designed and tested, only composites consisting of the donor poly[2-methoxy-5-(2-ethyl-hexyloxy)-(phenylene vinylene)] (MEH-PPV) and the acceptors PCBM- $C_{60}$  and a perylene-3,4,9,10-tetracarboxylic diimide derivative (PDI2) will be discussed here. These composite systems exhibited the most effective suppression of nanosecond laser pulses during our studies. This stands to reason since MEH-PPV is known to show strong two-photon absorption (2PA) in the near infrared (NIR) and both PCBM- $C_{60}$  and PDI2 possess anion absorption in this same wavelength region.

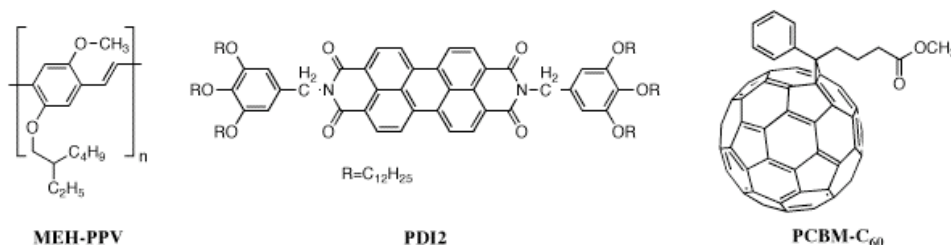


*Figure 1. Chemical structures of MEH-PPV, PDI2, and PCBM- $C_{60}$ .*

The processing of the CT composite films was chosen such that good optical quality, reduced transmission losses in the 700 - 900 nm range, and high concentrations of active components could all still be achieved. To obtain thick composite films melting was chosen as the primary processing method. Addition of plasticizer molecules that induce free volume in polymers, such as dioctylphthalate (DOP), can reduce melting and composite processing temperatures, improve processability and miscibility of two component systems, and reduce crystallinity in the resulting films. With 50 wt% of DOP, MEH-PPV CT composites were processed below 200°C into optical quality films with thicknesses ranging from 15 – 200  $\mu$ m and possessed good transparency from 700 to 900 nm (see Fig. 2).



*Figure 2. Microscope images (40x) of thick composites of MEH-PPV with different acceptors. (a) 25  $\mu$ m thick composite of MEH-PPV and PDI2. (b) 100  $\mu$ m thick composite of MEH-PPV and PDI2. (c) 25  $\mu$ m thick composite of MEH-PPV and PCBM- $C_{60}$ .*

Open aperture Z-scan measurements were performed using 70 fs pulses on these films and 2PA coefficients ( $\beta$ ) were determined. Average  $\beta$  values for the 700 – 900 nm region were found to be quite large for the MEH-PPV:PCBM- $C_{60}$  and MEH-PPV:PDI2 films:  $\sim 45$  cm/GW and  $\sim 23$  cm/GW, respectively. These values in conjunction with long lifetime CT states suggested efficient optical limiting was possible. Such studies were performed on the CT composite films in this spectral region with 7 ns pulses using a F/5 geometry and the results are shown in Figure 3. Both films possessed **linear transmittances of  $\sim 65\%$** , and the MEH-PPV/PCBM- $C_{60}$  film exhibited  **$\sim 15$  dB of suppression at 800 nm** with no catastrophic damage while the MEH-PPV:PDI2 film showed 11 dB of suppression at 750 nm. Adjustments to the constituent percentages of the films, modification of the optical limiting geometry, and use of single-shot excitation to increase the damage threshold should allow further improvements in suppression.

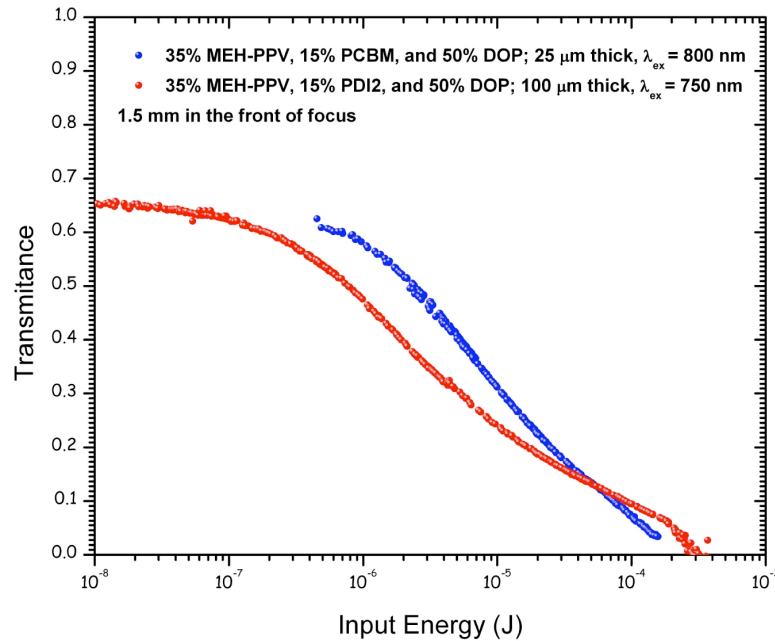


**Figure 3.** Optical power limiting studies performed with 7 ns pulses in a F/5 geometry on MEH-PPV CT films. Films were placed  $\sim 1.5$  mm before the focus.

It was pointed out (Augustine Urbas, *AFRL*) that proper optical limiting behavior must take into account fluence at the detector plane. Accordingly, beam shapes were measured at the focal plane during the optical limiting experiments described above with the 25  $\mu$ m MEH-PPV:PCBM- $C_{60}$  film positioned  $\sim 1$  mm in front of the focal plane. The beam size was found to be broadened by  $\sim 1.5$  times at high energy (50  $\mu$ J) compared to low energy (20 nJ). This resulted in a two times reduction of the fluence at the focal plane suggesting that the aforementioned suppression calculated using the total integrated energy is actually more pronounced. Even with this modest broadening, **the suppression for the CT film** would increase from  $\sim 15$  dB to  **$\sim 18$  dB at 800 nm**. Further optimization of beam spreading near the focus should serve as an additional route to improve optical limiting.

## B. Solution-Based Optical Limiting

As an alternative to film-based optical limiting, solutions were utilized which provided greater flexibility in terms of modifying the optical geometry. Two target organic systems are shown in Figure 4. CH-III-107 is a CT dyad complex, which obviates the need for high number density films by covalently attaching a perylene-3,4,9,10-tetracarboxylic diimide acceptor directly to an electron-rich, two-photon absorbing chromophore. YRS-I-30 is a squaraine system which has been shown to not only possess large 2PA cross-sections in the 700 – 900 nm spectral regime but also exhibits 2PA-induced excited-state absorption (ESA) as well.

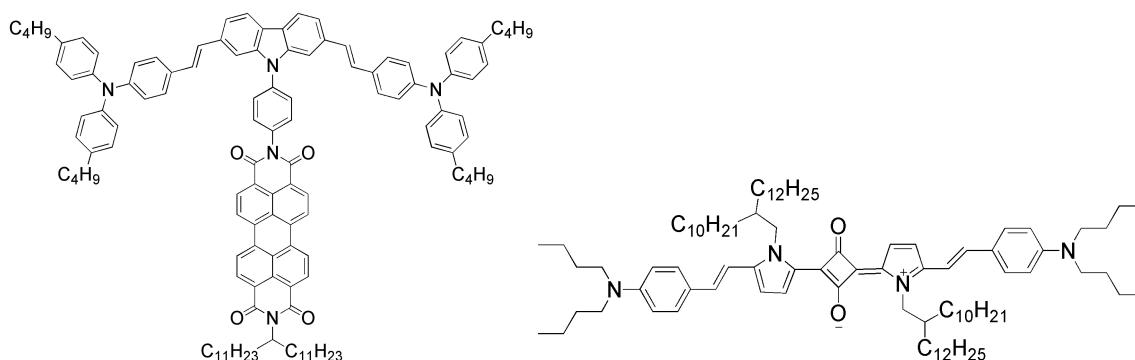


**Figure 4.** Chemical structures of CH-III-107 (left) and YRS-I-30 (right).

The results for nanosecond optical limiting studies (7 ns, F/5 geometry) on the aforementioned molecules in solution are given in Table 1. The suppression values are relatively modest due primarily to the limited dynamic range available following catastrophic optical damage to the cuvette containing the solution. Effective 2PA cross-sections ( $\delta$ , given in GM =  $1 \times 10^{-50} \text{ cm}^4 \text{-sec-photon}^{-1}$ ) as measured by femtosecond Z-scans are also given in the table and reveal quite sizable values in this spectral regime. These results suggest such solutions should offer a viable route to effective optical limiting provided a geometry could be chosen that would allow for greater suppression to occur prior to the onset of optical damage.

**Table 1.** Sample characteristics for solution-based nanosecond optical limiting on compounds given in Figure 4. Effective 2PA cross-sections as determined by femtosecond Z-scan are also given.

<b>Constitution</b>	<b><math>\delta_{eff}</math> (GM)</b>	<b><math>L</math> (mm)</b>	<b><math>\lambda</math> (nm)</b>	<b><math>T_L</math></b>	<b>Suppression<sup>C</sup></b>
CH-III-107 in chloroform <sup>A</sup>	2300 (730 nm)	1	750	0.87	4.8 dB (3x)
CH-III-107 in chlorobenzene <sup>B</sup>	2300 (730 nm)	10	750	0.74	11 dB (12.5x)
YRS-I-30 in toluene <sup>A</sup>	21,400 (870 nm)	1	850	0.74	5.9 dB (3.8x)

<sup>A</sup> Optical damage (~0.3 mJ) typically determined dynamic range for limiting, i.e.  $\min T_{NL}$

<sup>B</sup> No optical damage observed

<sup>C</sup> Suppression determined by  $(\min T_{NL})^{-1}$

## C. Microcapillary (MC)-Based Optical Limiting

A particular geometry that would be appropriate involves the use of MC's for in-filling of the solutions mentioned above. It has been shown<sup>1</sup> that optical limiting in MC's are enhanced compared to bulk samples due to strong confinement over longer interaction lengths. Initial

testing on MC arrays (*InCom*, 40  $\mu\text{m}$  well size, 0.5 mm x 0.5 mm area, 4 mm pathlength) as well as single MC's (*Polymicro*, 50  $\mu\text{m}$  ID, 370  $\mu\text{m}$  OD, 1.1 cm pathlength) revealed a number of issues associated with solution encapsulation, focusing, imaging, and optically induced damage and bubble formation. To resolve the encapsulation issues, appropriate sample holders were developed (see Figure 5). Furthermore, collaboration with the Naval Research Laboratory (Steven Flom) has provided a greater knowledge base to aid in dealing with the remaining issues. Developing an effective geometry incorporating MC's should result in significant increases in optical suppression for target solution-based materials.

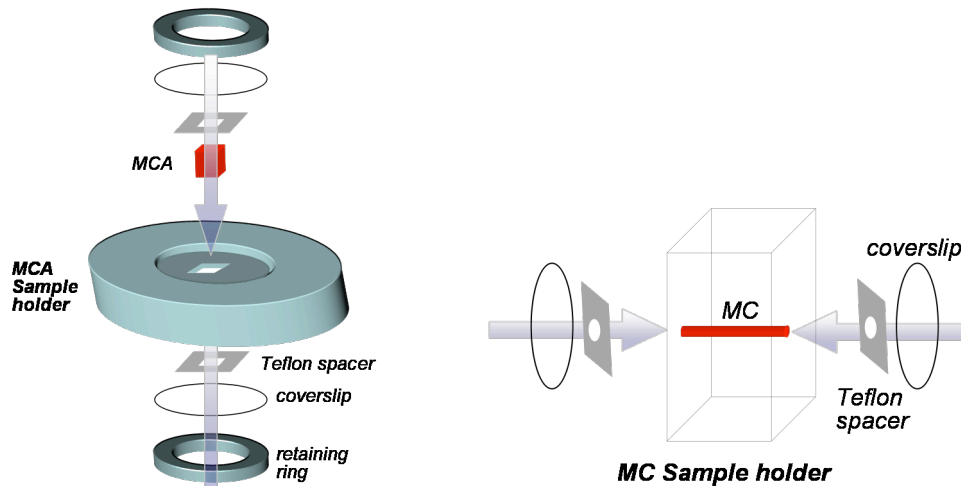


*Figure 5. Depiction of sample holders for microcapillary arrays (left) and single microcapillary tubes (right) to be used for solution-based optical limiting.*

#### **D. Nanoparticle Doped Bulk Liquid and Fiber Array Device**

Research in Prof. I.C. Khoo's group has been aimed at the use of a bulk liquid nonlinear material (L34) that is a 4-butyl, 4'-propyldiphenylacetylene compound and the doping of such liquid materials with silver and gold nanoparticles. These liquids and doped solutions have been used as nonlinear fillers in fiber array devices and the optical limiting performance has been investigated with  **$\sim 30 \mu\text{s}$  pulses at 750 nm**. The linear transmission of the L34 liquid is quite high across the visible and near-IR spectral regions as shown in Figure 6. The L34 neat liquid show a high **linear transmission of > 80% over the range of 700-900 nm**. The L34 filled fiber array shows a lower transmission due to the loss associated with the fiber array, which takes the transmission to about 50% at 800 nm. Figure 7 shows the imaging of an outdoor scene through an L34 filled fiber array. Figure 8 shows the optical limiting response of the L34 liquid doped with 2 nm gold nanoparticles and shows a suppression of **25 dB for  $\sim 30 \mu\text{s}$  pulses at 750 nm**.

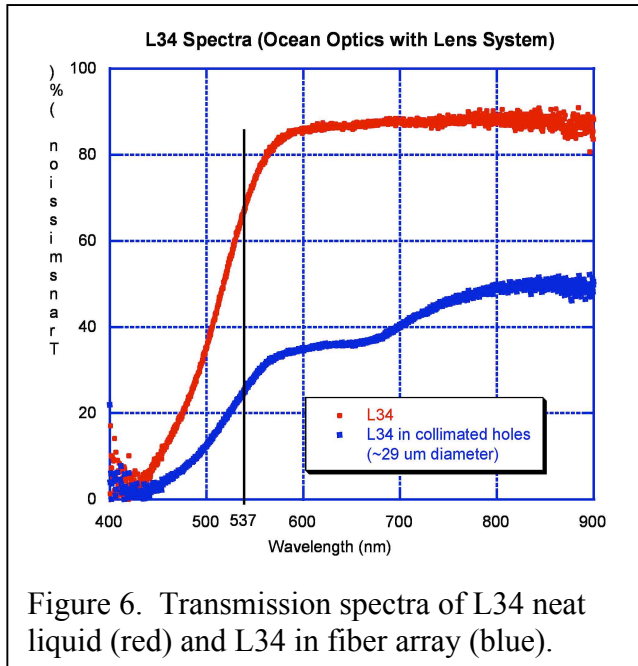


Figure 7. Image taken through fiber array filled with L34 neat liquid

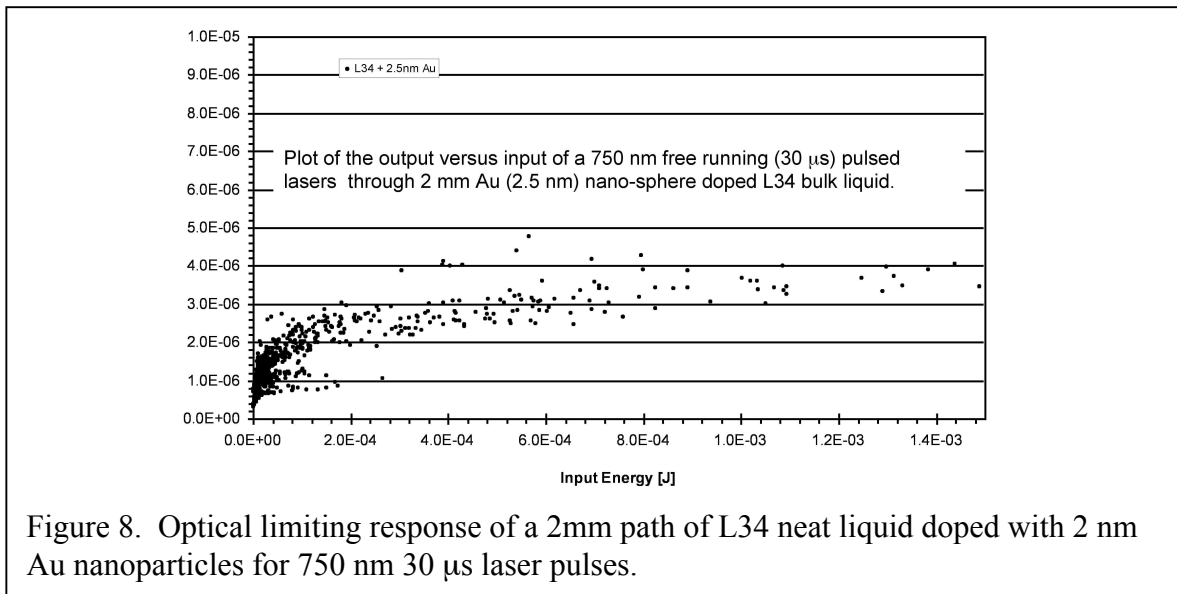


Figure 8. Optical limiting response of a 2mm path of L34 neat liquid doped with 2 nm Au nanoparticles for 750 nm 30 μs laser pulses.

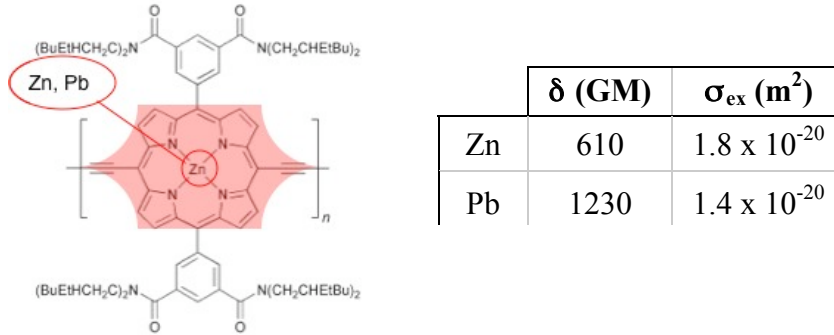
*Progress made toward the development of improved  $\chi^{(3)}$  materials for sensor protection in the 1530 – 1640 nm range (transmission > 60%, suppression of 20 dB, pulse duration ns – μs)*

### **E. Porphyrin Polymer Solutions**

The strong coupling of adjacent macrocycles in porphyrin bis-acetylide polymers has resulted in large optical nonlinearities at 1.06 μm<sup>ii</sup>. These studies suggested that such conjugated systems could be utilized for effective optical limiting in the 1530 – 1640 nm range. Accordingly, the

nonlinear optical properties of both a zinc and lead porphyrin polymer in solution, TEOSpol-Zn and TEOSpol-Pb (see Table 2 for chemical structures), were investigated. Solution absorption spectra revealed Q-band maxima at 780 and 858 nm, respectively, ensuring good optical transparency in the spectral region of interest. The microscopic nonlinearities of the two porphyrin polymers in solution were determined by femtosecond Z-scan and degenerate four-wave mixing (DFWM) at 1550 nm and are given in Table 2. The 2PA cross-sections were found to be  $> 600 \text{ GM}$  throughout the NIR regime. Furthermore, femtosecond transient absorption studies revealed that 2PA-induced ESA exists in this spectral regime as well. High irradiance Z-scan measurements allowed for extraction of ESA cross-section values ( $\sigma_{\text{ex}}$ , see Table 2) which were found to be  $> 500$  times the ground state absorption cross-sections at this wavelength. The order of magnitude difference in the ESA lifetimes between the polymers,  $\sim 0.3 \text{ ns}$  and  $\sim 4.0 \text{ ns}$  for TEOSpol-Zn and TEOSpol-Pb, respectively, could potentially be attributed to the different excited state manifolds (singlet or triplet) in which ESA takes place.

**Table 1.** Nonlinear optical properties for porphyrin polymers in solution. The chemical structures of the polymers are given on the left.



Optical power limiting studies were performed at **1550 nm** in both the femtosecond ( $\sim 70 \text{ fs}$ ) and nanosecond ( $\sim 7 \text{ ns}$ ) regimes (see Figure 6). The solutions had the following **linear transmittances: Zn  $\rightarrow$  0.91, Pb  $\rightarrow$  0.95 for fs; Zn  $\rightarrow$  0.90, Pb  $\rightarrow$  0.90 for ns.** The **optical suppression (in dB)** for each system, defined as  $(\min T_{\text{NL}})^{-1}$ , was as follows: Zn  $\rightarrow$  **12.4, Pb  $\rightarrow$  12.7** for fs; Zn  $\rightarrow$  4.7, Pb  $\rightarrow$  7.2 for ns. In each case, the Pb polymer outperformed the Zn polymer. In the fs regime, this was likely the result of an enhanced 2PA cross-section, and in the ns regime, probably the result of the longer excited-state lifetime.

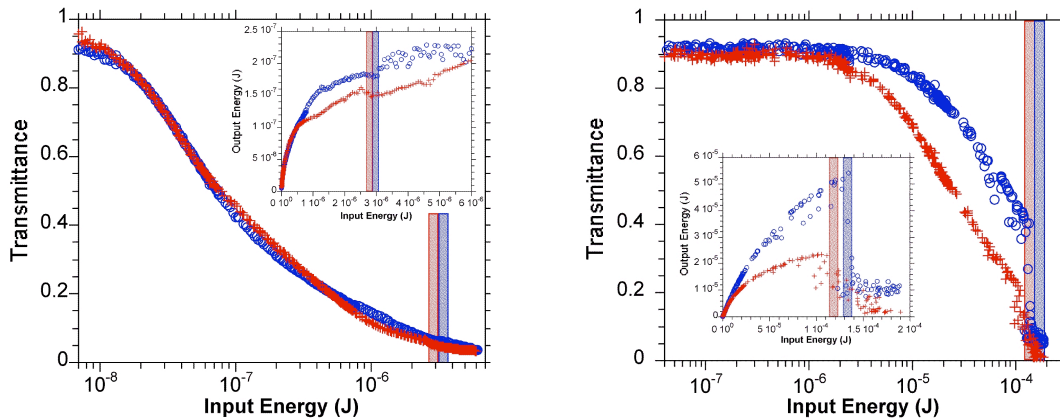




**Figure 6.** Optical power limiting studies performed with (a) ~70 fs and (b) ~7 ns pulses in a F/5 geometry on solutions of TEOSpol-Zn (open circles) and TEOSpol-Pb (crosses) in 1 mm cuvettes. Insets show output energy versus input energy and dark bars represent energies at which optical damage occurred.

### **F. Extended Squaraine – A Neat Liquid**

An additional chromophore has shown promise for liquid-phase optical limiting in the 1530 – 1640 nm range. This squaraine of extended conjugation, YRS-I-80 (Figure 7), exists as a neat liquid at room temperature and shows reasonable transparency in the spectral region of interest. This system has been shown to possess a large 2PA coefficient at 1550 nm<sup>iii</sup> and has also been shown to exhibit 2PA-induced ESA as well. Femtosecond optical limiting at **1550 nm** in an F/5 geometry for a 200  $\mu\text{m}$  cell filled with the neat liquid ( $T_L = 67\%$ ) showed **> 12 dB of suppression**. This system was also tested using picosecond excitation (Augustine Urbas, *AFRL*) and effective optical limiting was also observed. It should be noted that either of these two final sets of materials (porphyrin polymers or squaraine) in solution are candidates to be used in the MC geometries described above and therefore the promise of enhanced optical suppression exists.

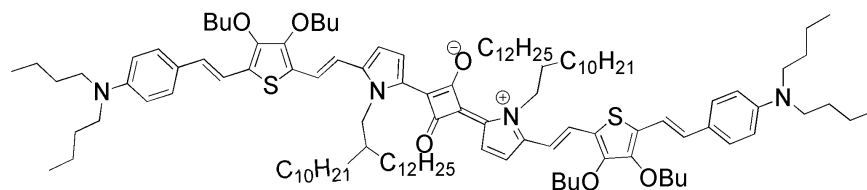


**Figure 7.** Chemical structure of YRS-I-80.

### **G. Conclusion**

The results presented above demonstrate that that we have met the major metrics for Phase II for  $\chi^{(3)}$  materials performance and sensor protection in the near infrared spectral region. We will utilize the approaches and materials developed in Phase II to move forward to developing limiter geometries that can make best use of these systems and put us into position for meeting the Phase III metrics.

---

### **H. References**

- <sup>i</sup> Butler, J. J., Wathen, J. J., Flom, S. R., Pong, R. G. S., Shirk, J. S., *Opt. Lett.*, **28**, 1689-1691 (2003).
- <sup>ii</sup> Screen, T. E. O., Thorne, J. R. G., Denning, R. G., Bucknall, D. G., Anderson, H. L., *J. Mat. Chem.*, **13**, 2796-2808 (2003).
- <sup>iii</sup> Chung, S.-J. *et al.*, *J. Am. Chem. Soc.*, **128**, 14444-14445 (2006).